Preparation of Ammonia Dealuminated Metakaolinite and Its Adsorption against Bixin

Winda Rahmalia[1], Jean-François Fabre[2], Thamrin Usman[1,*], and Zéphirin Mouloungui[2,3]

[1]*Department of Chemistry, Faculty of Mathematics and Natural Sciences, Tanjungpura University,*
Jl. Prof. Dr. H. Hadari Nawawi, Pontianak 78124, West Kalimantan, Indonesia

[2]*Université de Toulouse, INP-ENSIACET, Laboratoire de Chimie Agro-industrielle (LCA),*
4 Allée Emile Monso, 31030 Toulouse, France

[3]*INRA, UMR 1010 CAI, F-31030 Toulouse, France*

Abstract: *This study aims to prepare dealuminated metakaolinite which has a high surface area by using NH_4OH as an activator. The natural kaolinite sample was treated at 600 °C for 6 h in order to obtain metakaolinite. A dealuminated metakaolinite was then prepared by the repeated activation method using concentrated ammonia (5 M NH_4OH) at room temperature. Depending on the nature of each type of material, natural kaolinite, NH_4OH treated kaolinite, metakaolinite and NH_4OH treated metakaolinite were characterized using X-ray diffraction (XRD), Fourier-transform infrared spectroscopy (FTIR), scanning electron microscopy-energy dispersive spectroscopy (SEM-EDS), and Brunauer-Emmett-Teller (BET-N_2) measurements. XRD and FTIR results confirmed that structural transformation from kaolinite to metakaolinite had occurred. According to SEM-EDS data, the activation of metakaolinite by NH_4OH allowed the dealumination of metakaolinite. The increase in the Si/Al ratio was almost twice as high as in kaolinite. BET-N_2 analysis showed that the specific surface area and the total pore volume increased significantly after activation. Its adsorption properties were tested against bixin. Bixin adsorption on dealuminated metakaolinite followed pseudo-second order kinetic where $k_2 = 0.20$ g/mg min. The adsorption isotherm followed the Langmuir model where qm = 0.72 mg/g.*

Keywords: *ammonia; adsorption; bixin; metakaolinite*

■ INTRODUCTION

Kaolinite [$Al_2Si_2O_3(OH)_4$] is a mineral clay that is relatively inexpensive. It is effective as a support material. This behavior is governed by the extent and nature of the outer surface, the interspace, and the crystal structure that can be modified by appropriate processing techniques [1-3]. Acidic or alkaline activation has been widely studied as a chemical treatment to improve the characteristics of natural kaolinite. However, activation from natural kaolinite shows that improving the properties of kaolinite by chemical processes is difficult because of the high passivity of this material. Thus, it was not significantly affected by acidic or alkaline treatments, even under concentrated solution conditions [4-7].

Due to the passivity of kaolinite, acidic or alkaline activation was also studied from metakaolinite. It is a metastable phase obtained by calcination of kaolinite, which has been reported to be more reactive in chemical treatments. Metakaolinites are obtained by calcination of kaolinite at temperatures between 500 and 900 °C [5,8]. This transformation occurs by losing its structural water and a reorganization of the structure. Only a small part of AlO_6 octahedron is maintained, while the rest is transformed into much more reactive tetra and pentacoordinate units. This process of dehydroxylation is presented in following equation [5].

$$Al_2O_3(SiO_2)_2(H_2O)_2 \text{ (kaolinite)} \rightarrow Al_2O_3(SiO_2)_2(H_2O)_x + (2-x)H_2O \uparrow$$
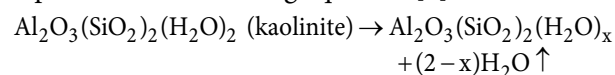
The calcination conditions of kaolinite strongly influence the reactivity of the solids obtained. The best conditions for obtaining a highly reactive metakaolinite were discussed by various authors who reported calcination values between 600 and 800 °C [5,9-10]. Calcination at higher temperatures leads to the formation of mullite and cristobalite. In this study, we used the calcination temperature of 600 °C according to the adapted protocol written by Belver et al. [5].

Rahmalia et al. [6] previously studied the characterization of HCl and KOH treated kaolinite and their adsorption properties against bixin (Fig. 1). The results showed that there was only little change in the kaolinite structure after treatment. However, the activation of kaolinite using alkaline solutions allowed the increase of the adsorption capacity of bixin, both isotherms adsorptions, and kinetics. Bixin was chosen in this study because it is a carotenoid dye that is widely used in industry, cosmetics, pharmaceutical products, as food coloring, textile dye [11-14], sensitizer in the solar cell [15-17] and photodynamic therapy [18]. The double bonds structure of bixin renders it unstable to light, temperature, and oxygen exposure [19-20]. Incorporating bixin into the surface or interlayer space of clay minerals is one of the efforts to increase its stability [21-22].

In line with the development of environmentally friendly technologies, NH_4OH is a less toxic alternative to KOH. KOH strongly attacks cell constituents by dissolving keratin, hydrolyzing lipids, and degrading proteins. The destructive effect of KOH on the eyes is particularly serious. The effect of NH_4OH is less severe. The corrosive effects of NH_4OH cause destruction of single tissues, while KOH causes severe tissue destruction [23]. NH_4OH enters the nitrogen cycle. It is produced in the soil by bacterial methods. NH_4OH is also produced naturally from the decomposition of organic matter [24]. So we used NH_4OH in this work. Since the alkaline properties of NH_4OH are almost the same as KOH, it is advantageous to develop a new activator which has less toxicity, and is believed to also improve surface properties of natural kaolinite.

Although the bixin adsorption rate on kaolinite is faster when acetone acts as a solvent, it is preferred to use dimethyl carbonate (DMC) since it can increase the adsorptive capacity of bixin on kaolinite [6]. Most properties of DMC make it a truly green reagent [25]: (1) DMC is a non-toxic compound. Since the mid-1980s, it is no longer produced from phosgene, but rather by oxidative catalytic carbonylation of methanol with oxygen. In addition to improving the safety of the procedure, this manufacturing process avoids phosgene contamination and eliminates the need for inorganic salts as by-products. (2) DMC is classified as a flammable liquid just like methanol, and has no irritant or mutagenic effects, either by contact or by inhalation. Therefore, it can be handled safely without the special precautions required for toxic and mutagenic methyl halides. (3) DMC has a versatile and flexible chemical reactivity that depends on experimental conditions.

Thus, the objective of this work is the activation of metakaolinite using concentrated NH_4OH solution to obtain the metakaolinite with better properties. The treatment of kaolinite using concentrated NH_4OH was also done for comparative study. The parameters studied are the properties of kaolinite and metakaolinites after activation and its adsorption characteristics against bixin.

■ EXPERIMENTAL SECTION

Materials

Bixin crystals containing 88.11% *cis*-bixin and 11.75% di-*cis*-bixin and an unknown compound (0.14%) were obtained by the extraction and purification processes described by Rahmalia et al. [26]. Natural kaolinite ($Al_2O_7Si_2 \cdot 2H_2O$), CAS Number 1318-74-7, was supplied by Sigma-Aldrich (Germany), together with analytical grade ammonium hydroxide (NH_4OH, NH_3 28.0–30.0%) and dimethyl carbonate (99%) were supplied by Sigma-Aldrich, Germany.

Procedure

Preparation and activation of metakaolinite by NH4OH

The kaolinite was calcined at 600 °C in an oven to give the corresponding metakaolinite. The calcination was carried out under an air atmosphere in a programmable furnace, with a program for heating from

room temperature to the calcination temperature by 10 °C min^{-1} and maintaining the calcination temperature for 6 h. The metakaolinite obtained was named K_{Cal}. Activation was performed by adding 10 g of K_{Cal} in 100 mL of a 5 M NH_4OH solution. The mixture was stirred on a vibrating table continuously (300 rpm) for 6 h at room temperature. The suspension was filtered and the residue was washed using distilled water until neutral and dried in an oven at 103 °C for 24 h. This process was repeated 3 times to optimize the activation process. The final product obtained was called K_{CA}. The activation of kaolinite without calcination was also done by a similar method, and the final product obtained was called K_A. K_A, K_{Cal}, and K_{CA} were characterized by XRD, FTIR, SEM-EDS, and BET-N$_2$.

Adsorption of bixin on KB and KCA

The adsorption process was carried out by adopting the experiment optimum condition of Rahmalia et al. [6]. Stock solutions of bixin (20 mg/L) were prepared in dimethyl carbonate. Solutions at the required concentrations (3–18 mg/L) were prepared by dilution of the stock solution. The adsorbent (0.05 g) was then added to a solution of 5 mL of bixin (3–18 mg/L). The mixtures were stirred on a vibrating table continuously (300 rpm) at room temperature (~22 °C). Samples were taken after 4 h (predetermined equilibrium time) and small aliquots of the supernatant were removed and diluted to an appropriate concentration, if necessary. The absorption spectrum was determined immediately with a Shimadzu UV-1800 UV-visible spectrophotometer. Concentrations of bixin in the solutions were determined by a UV-visible spectrophotometer calibrated at 456 nm dimethyl carbonate [27]. For contact time studies, the residual concentration of 5 mL of bixin solution (10 mg/L) with kaolinite (0.1 g) was determined at various time points from 5 to 360 min. The experiments were performed in triplicate and mean values were reported.

■ RESULTS AND DISCUSSION

Characteristics of Dealuminated Metakaolinite

The XRD diffractograms (Fig. 1) show the amorphous patterns for K_{Cal} and K_{CA}. The calcination process resulted in significant crystallographic transformations of kaolinite.
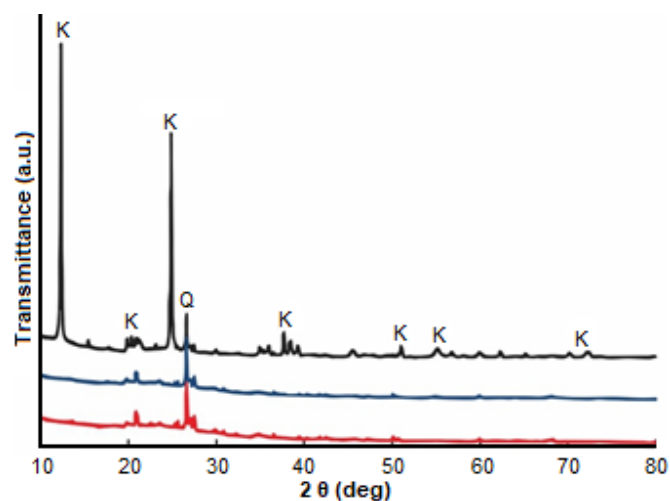
Fig 1. XRD diffragtograms of K_A (black), K_{Cal} (blue), and K_{CA} (red)

Two intense diffraction reflections at 2θ values of 12.3 and 24.9° which were observed at K_A had disappeared, while peaks attributed to quartz (2θ of 21.22 and 27.45°) remained unchanged. A diffractogram for K_A showed no significant difference with respect to kaolinite before activation as reported in Rahmalia et al. [6]. The calcination product patterns are similar to those reported for metakaolinites [5,9]. Since the activation of metakaolinite was performed at room temperature, the XRD pattern of K_{CA} did not show significant variations from K_{Cal}. This indicates that treatment with NH_4OH at room temperature leads to very small alterations in the crystal structure of metakaolinite. However, the International Centre for Diffraction Data (ICDD) shows that K_{CA} (PDF 01-076-5970) contains a small amount of sodium aluminum silicon oxide. It is the precursor component of zeolite formation. This mineral is not present in the K_{Cal}. This result shows that NH_4OH has the ability to convert metakaolinite to zeolite although activation was performed at room temperature.

FTIR analysis (Fig. 2) confirm the transformation of kaolinite during calcination and activation. The FTIR spectra patterns of K_A showed no significant differences between kaolinite before and after treatment, indicating an absence of significant change in the kaolinite samples. The FTIR spectrum of natural kaolinite published by Rahmalia et al. [6] was also presented for comparison. The FTIR spectrum of natural kaolinite characteristic bands
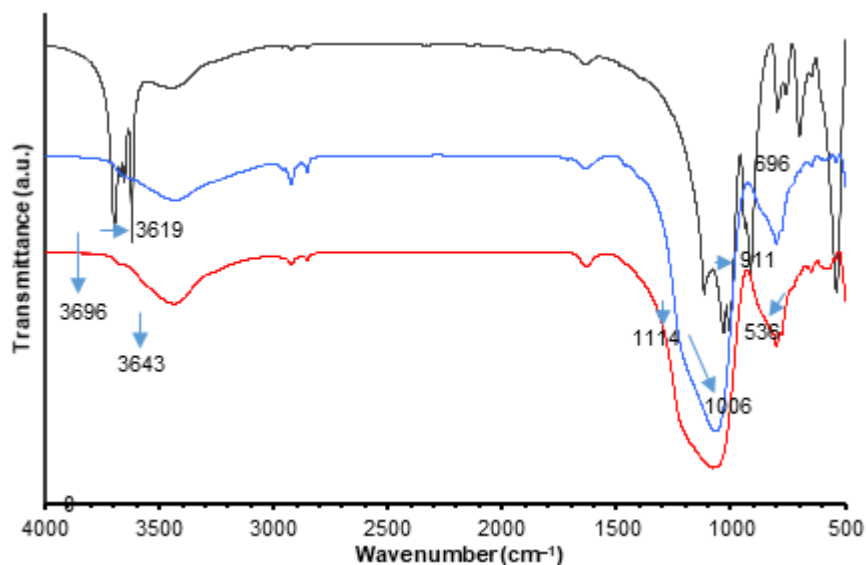
Fig 2. The FTIR spectra of K_A (black), K_{Cal} (blue), K_{CA} (red)

of kaolinite: at 3696, 3669, 3652, and 3619 cm^{-1} correspond to the stretching of inner-surface-hydroxyl groups, at 3443 cm^{-1} corresponds to stretching of the hydroxyl group of water, 1631 cm^{-1} corresponds to the O–H deformation of water, 1114 cm^{-1} corresponds to Si–O stretching (longitudinal mode), 1030, and 1006 cm^{-1} correspond to in-plane Si–O stretching, 937 cm^{-1} corresponds to the –OH deformation of inner-surface hydroxyl groups, 911 cm^{-1} corresponds to Al–OH deformation, 794 cm^{-1} corresponds to Si–O vibration, 755 and 696 cm^{-1} correspond to Si–O perpendicular vibrations, 536 cm^{-1} corresponds to Al–O–Si deformation, 468 cm^{-1} corresponds to Si–O–Si deformation, and 428 cm^{-1} corresponds to Si–O deformation.

The calcination process of kaolinite caused the almost complete disappearance of the water and hydroxyl bands. The stretching of inner-surface-hydroxyl groups bands at 3696, 3669, 3652 and 3619 cm^{-1}, and the –OH deformation of inner-surface hydroxyl groups band at 937 cm^{-1} also disappeared. This proves that the dehydroxylation process occurred. The significant decrease in Al–OH deformation band at 911 cm^{-1} and Al–O–Si deformations at 536 cm^{-1} indicates that the evolution of octahedral Al^{3+} coordination in the kaolinite structure towards coordination tetrahedral in metakaolinite was observed.

The spectrum of metakaolinite shows a very simple spectrum, consisting of three broad bands centered at 1079, 777, and 470 cm^{-1}. The first corresponds to the vibrations of the tetrahedral sheet, clearly showing the deformation of this sheet during calcination. The second band corresponds to silica or free quartz, unaffected by calcination. Finally, the third band corresponds to the structural flexural vibrations. The simplification of this region also shows the structural deformation of kaolinite in metakaolinite.

Glukhovsky et al. [28] proposed a general mechanism for the alkaline activation of materials consisting mainly of silica and reactive alumina. The mechanism of the Glukhovsky model is composed of joint destruction-coagulation-condensation-crystallization reactions. The first step is a decomposition of the Si–O–Si and Al–O–Si covalent bonds, which occurs as the pH of the alkaline solution increases. These groups are therefore transformed into a colloidal phase. Then, an accumulation of destruction products occurs, which often interacts with each other to form a coagulated structure, which leads to the third phase, the generation of a condensed and crystallized structure. In another study, Steinerova [29] reported that metakaolinite in a strong alkaline medium allows hydrolysis of metakaolinite source components and their disintegration during which bridging oxygen (BOS) converses to non-bridging oxygen (NBOs) precursors release (BOS → NBOs), leading to a solution of the hydrated units of SiO$_4$ and AlO$_4$. As a consequence, we did not observe any significant

differences between the IR spectra of K_{CA} and K_{Cal}. On the other hand, the Al–O–Si deformation band at 536 cm^{-1} completely disappeared, followed by the decrease in intensity of the Si–O–Si band at 468 cm^{-1}.

Alkaline attack on the structure of metakaolinite produces a release of silicate and aluminate species in solution, with 5 or 6 Al coordinates converted into 4-coordinations during dissolution. In this case, the release of Al may be faster than that of Si [30]. This can be explained by the decrease in the percentage of Al in metakaolinite after activation as observed by elemental analysis using SEM-EDS (Table 1). According to SEM-EDS data, the activation of metakaolinite by NH$_4$OH allowed the dealumination of metakaolinite. The increase in the Si/Al ratio was almost twice as high as in natural kaolinite, K_A and K_{Cal}.

Table 2 shows that monolayer volume, surface area, and total pore volume decreased during calcination due to particle aggregation when water molecules was removed from the structure. Meanwhile the average pore diameter showed an increase, indicating that the high temperature calcination process also allowed pore opening by minimizing organic contaminations of natural kaolinite. The specific surface area and the total pore volume increased significantly after treatment for K_{CA} because of the reorganization of the K_{Cal} structure. These results show that metakaolinite is more reactive under treatment compared to natural kaolinite. NH$_4$OH is capable of activating kaolinite by increasing slightly the surface area and average pore diameter of K_A. NH$_4$OH was capable of dealuminating metakaolinite by increasing the surface area by up to 16 times more than natural kaolinite. It is

probably due to the ability of concentrated NH$_4$OH to dissolve aluminic and silicic part of metakaolinite.

Due to the change in chemical composition, the mapping of the elements was conducted for natural kaolinite and K_{CA} using SEM-EDS with a magnification of 2000× to know their distributions of chemical elements. The results of the analyses are shown in Fig. 3. It is found that the elements of O, N, Mg, Al, Si, and K of natural kaolinite were homogenously distributed. After calcination followed by activation, a new phase was observed forming more pores. Activation by NH$_4$OH lead to the formation of pore domains that were larger in the clusters site of chemical elements such as O, Si, and Al. This figure also shows the change in the distribution of the chemical elements of Na, Mg, and K but less important.

Adsorption of Bixin on Dealuminated Metakaolinite

For the comparison study with respect to natural kaolinite, HCl treated kaolinite, and KOH treated kaolinite, that Rahmalia et al. [6] had studied previously, we carried out the adsorption of bixin on K_A and K_{CA}

Table 1. SEM-EDS analysis data

Element	wt.%			
	Natural kaolinite [11]	K_A	K_{Cal}	K_{CA}
O	56.9	58.0	53.3	56.0
Na	0.42	0.45	0.29	0.37
Mg	0.15	0.26	0.31	0.19
Al	18.4	18.2	19.8	13.7
Si	23.1	22.5	24.5	28.1
K	0.79	0.38	0.72	0.83
Fe	0.22	0.22	0.22	0.23
Si/Al	1.26	1.23	1.24	2.06

Table 2. BET-N$_2$ analysis data

| Kaolinites		Natural kaolinite [11]	K_A	K_{Cal}	K_{CA}
Weight of sample (g)		0.21	0.22	0.21	0.19
Saturation vapor pressure (kPa)		99.22	99.78	97.18	97.14
BET Parameters Analysis	Volume of monolayer, V_m (cm^3 STP g^{-1})	1.76	1.88	1.64	28.57
	Constant of energy, C (first layer)	42.94	35.99	122.07	2877.50
	Surface area BET, a_s BET (m^2 g^{-1})	7.65	8.15	7.13	124.33
	Total pore volume, $p/p_0 = 0.99$ (10^{-2} cm^3 g^{-1})	3.62	2.89	2.34	7.43
	Average pore diameter, d_p (nm)	8.20	14.17	13.16	2.39
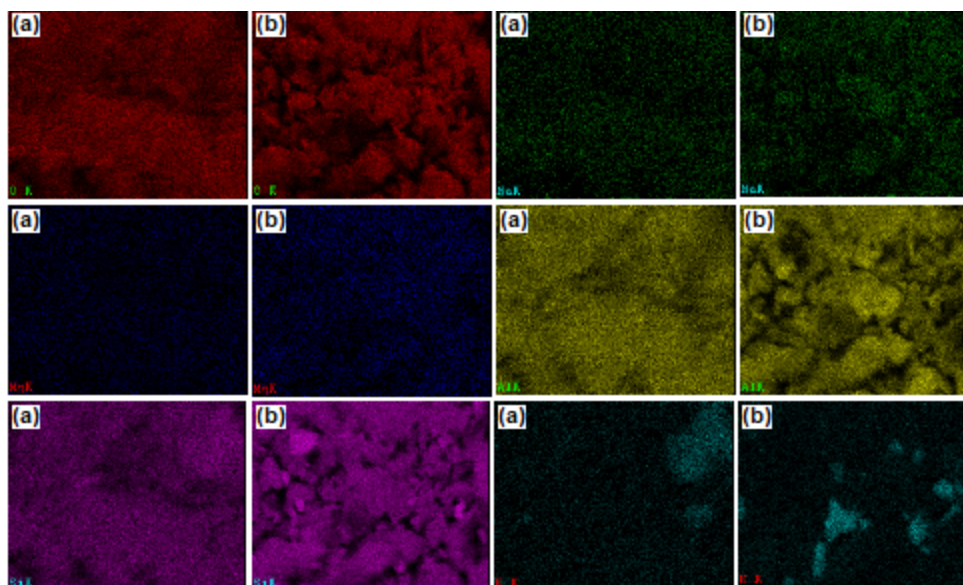
Fig 3. Cartography of elements of natural kaolinite (a) and K_{CA} (b)

using dimethyl carbonate as the solvent. The effect of contact time showed that bixin in dimethyl carbonate needed 240 min to wait for equilibrium (Fig. 4). The result was the same when natural kaolinite, HCl treated kaolinite, and KOH treated kaolinite were used as adsorbents.

The absorption spectrum of the supernatant solution of bixin in dimethyl carbonate before and after adsorption by K_A and K_{CA} for 240 min is shown in Fig. 5. In contrast to the adsorption properties of bixin on natural kaolinite and treated kaolinite, the spectrum of bixin after adsorption on K_{CA} showed a small red displacement (bathochromic). It appeared in the visible region and gave a maximum absorbance at 462 nm, moving 6 nm with respect to the bixin spectrum before adsorption (456 nm), and is associated with the position of the 0–1 band of vibrations. This behavior is an advantage in bixin applications as a photosensitizer. That is, less energy is needed for the bixin to be excited from HOMO to LUMO compared to bixin adsorbed on natural kaolinite and treated kaolinite.

In order to explain the design of an adsorption system and the interaction between bixin and metakaolinite in this study, we used the most common types of isotherms, which are the Langmuir and Freundlich models. They are the best models to explain the trend of adsorption based on the essence of absorbents saturated with adsorbate after
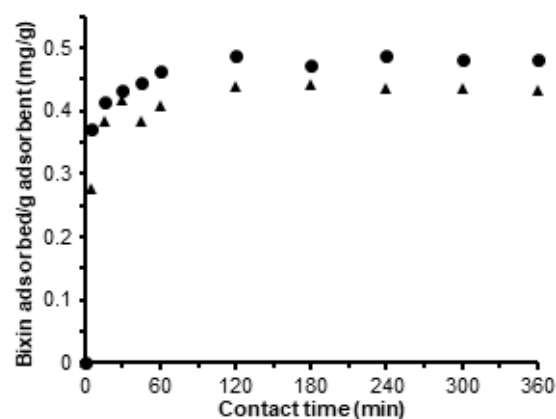

Fig 4. Effect of contact time on adsorption of bixin using K_A (▲) and K_{CA} (●)
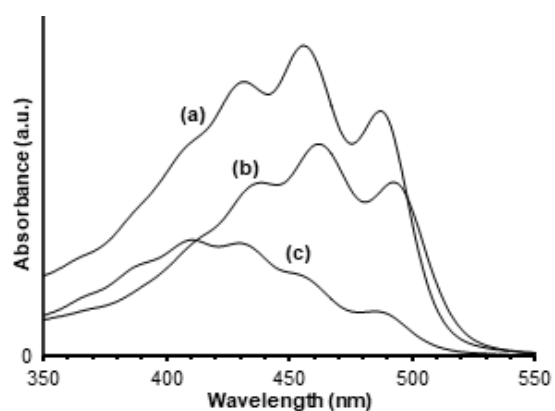

Fig 5. Supernatant solution absorption spectrum of bixin in dimethyl carbonate before (a) and after adsorption on K_A (b) and K_{CA} (c)

enough contact time. Freundlich isotherm is applicable to adsorption processes that occur on heterogonous surfaces. This isotherm gives an expression which defines the surface heterogeneity and the exponential distribution of active sites and their energies. The linear form of the Freundlich isotherm is as follows [31]:

$$\log q_e = \log K_f + \frac{1}{n} \log C_e \tag{1}$$

where q_e is the amount of the adsorbate at equilibrium (mg/g), C_e is the equilibrium concentration of the adsorbate on the adsorbent (mg/L), K_f is adsorption capacity (L/mg) and $1/n$ is adsorption intensity; it also indicates the relative distribution of the energy and the heterogeneity of the adsorbate sites.

In the Langmuir model, the mass of solute adsorbed per unit mass of adsorbent increases linearly with solute concentration at low surface coverage, approaching an asymptote as the adsorption sites become saturated. Eq. (2) is based on three important assumptions: (1) the energy of adsorption is identical for all sites and is independent of surface coverage, (2) adsorption occurs only at localized sites, with no interaction between adjoining adsorbed molecules, and (3) the sorption maximum represents monolayer coverage. The linear form of the Langmuir Eq. (2) can be expressed as follows [32]:

$$\frac{C_e}{q_e} = \frac{1}{K_L \cdot q_m} + \left(\frac{1}{q_m}\right) C_e \tag{2}$$

where K_L is Langmuir constant related to adsorption capacity (mg/g), which can be correlated with the variation of the suitable area and porosity of the adsorbent which implies that large surface area and pore volume will result in higher adsorption capacity, and q_m is maximum adsorption capacity (mg/g).

Table 3 shows that the equilibrium data did not correspond to the Freundlich equation for K_A and K_{CA} in dimethyl carbonate. The poor fit of these models was demonstrated by the very low correlation coefficient ($r^2 < 0.95$) and the values of $n > 1$. The Langmuir equation gave a better fit, with $r^2 > 0.95$. This indicates the presence of a homogeneous active site and the coverage of the adsorbent surface with a monolayer of bixin. Depending on the values of q_m, the bixin adsorption on K_{CA} is favorable compared to K_A. This is predictable as the adsorption capacity of adsorbents increased with an increase in the specific surface area of BET.

The adsorption kinetics (k_1 and k_2) were also calculated for K_A and K_{CA} as well as the correlation coefficient, the values of q_{e1} and q_{e2} (calculation) and q_e (experiment) by using the Lagergren's pseudo-first order and pseudo-second order models to investigate the

Table 3. Adsorption parameters for the adsorption of bixin on K_A and K_{AC}

Adsorption isotherm parameters		K_A	K_{AC}
Freundlich	K_f (L/mg)	0.36	0.60
	N	0.14	8.76
	r^2	0.42	0.30
Langmuir	K_L (mg/g)	7.89	6.16
	q_m (mg/g)	0.47	0.72
	r^2	0.99	0.98
Adsorption kinetic parameters		K_A	K_{AC}
Pseudo-first order	q_e exp (mg/g)	0.44	1.43
	q_{e1} (mg/g)	0.19	0.46
	k_1 (10^{-2}) (1/min)	3.57	10.4
	r^2	0.84	0.73
Pseudo-second order	q_{e2} (mg/g)	0.44	1.41
	h (10^{-2}) (mg/g min)	20.1	39.9
	k_2 (mg/g.min)	1.05	0.20
	r^2	0.99	0.99

dynamics of the bixin adsorption process. The pseudo-first order model assumes that the rate of change of solute uptake over time is directly proportional to the difference in saturation concentration and the amount of solid uptake over time. In most cases, the adsorption reaction involves diffusion across a boundary (3) [33]. The adsorption process with chemisorption controls the rate, according to the pseudo-second order model (4) [34].

$$\log\left(q_e - q_t\right) = \log q_e - k_1 \cdot \frac{t}{(2.303)'} \qquad (3)$$

$$\frac{t}{q_t} = \frac{1}{(k_2 q_e^2)} + \left(\frac{1}{q_m}\right) \cdot t \qquad (4)$$

where k_1 is pseudo first order adsorption rate constant (1/min) and k_2 is pseudo second order adsorption rate constant (g/mg min). Values of k_1 and k_2 were calculated from the intercept of the corresponding plots of log (q_e – q_t) against t and t/q_t against t.

As seen in this table, the values of the correlation coefficients for the pseudo-second-order rate equation were found to be higher than those of the pseudo-first-order rate equation. Although the r^2 values for plots are in the range of 0.7329 after applying the pseudo-first order model, the calculated q_{e1} values obtained from this model do not give reasonable values because they are very small relative to the values of the experimental q_e. The values of q_{e2} and q_e were close in agreement with the other values for the pseudo-second order model. These results confirm that the bixin adsorption process on both K_A and K_{CA} follow the pseudo-second-order kinetic model. These results prove that adsorption occurs in this experiment by chemisorption [35].

CONCLUSION

The treatment of metakaolinite with NH_4OH is a good method for producing the dealuminated metakaolinite with a very large surface area. The nature of the adsorption process depends on the physical and chemical characteristics of the adsorbents, as well as on the conditions of the system. The product obtained can also slightly decrease the energy required to excite the electrons of the bixin from HOMO to LUMO. It can also increase the capacity of kaolinite to adsorb bixin to almost twice the amount of activated kaolinites without an initial calcination phase. Finally, dimethyl carbonate has potential to be a good solvent for increasing the adsorptive capacity of bixin on kaolinite.

REFERENCES

[1] Frost, R.L., Makó, É., Kristóf, J., and Kloprogge, J.T., 2002, Modification of kaolinite surface through mechanochemical treatment-a mid-IR and near-IR spectroscopic study, *Spectrochim. Acta, Part A*, 58 (13), 2849–2859.

[2] Frost, R.L., Kristóf, J., Makó, É., and Horváth, E., 2003, A DRIFT spectroscopic study of potassium acetate intercalated mechanochemically activated kaolinite, *Spectrochim. Acta, Part A*, 59, 1183–1194.

[3] Khan, T.A., Khan, E.A., and Shahjahan, 2015, Removal of basic dyes from aqueous solution by adsorption onto binary iron-manganese oxide coated kaolinite: Nonlinear isotherm and kinetics modeling, *Appl. Clay Sci.*, 107, 70–77.

[4] Kumar, S., Panda, A.K., and Singh, R.K., 2013, Preparation and characterization of acid and alkaline treated kaolin clay, *Bull. Chem. React. Eng. Catal.*, 8 (1), 61–69.

[5] Belver, C., Bañares-Muñoz, M.A., and Vicente, M.A., 2002, Chemical activation of kaolinite under acid and alkaline conditions, *Chem. Mater.*, 14 (5), 2033–2043.

[6] Rahmalia, W., Fabre, J.F., Usman, T., and Mouloungui, Z., 2018, Adsorption characteristics of

bixin on acid- and alkali-treated kaolinite in aprotic solvents, *Bioinorg. Chem. Appl.*, 2018, 3805654.

[7] Yahaya, S., Jikan, S.S., Badarulzaman, N.A., and Adamu, A.D., 2017, Effect of acid treatment on the SEM-EDX characteristics of kaolin clay, *Path Sci.*, 3 (9), 4001–4005.

[8] Mackenzie, R.C., 1970, Differential Thermal Analysis, Vol. I, Academic Press, London.

[9] Ilić, B.R., Mitrović, A.A., and Miličić, L.R., 2010, Thermal treatment of kaolin clay to obtain metakaolin, *Hem. Ind.*, 64 (4), 351–356.

[10] Varga, G., 2007, The structure of kaolinite and metakaolinite, *Epítöanyag*, 59, 6–9.

[11] Cardarelli, C.R., Benassi, M.T., and Mercadante, A.Z., 2008, Characterization of different annatto extracts based on antioxidant and colour properties, *LWT Food Sci. Technol.*, 41 (9), 1689–1693.

[12] Das, D., Maulik, S.R., and Bhattacharya, S.C., 2007, Dyeing of wool and silk with *Bixa orellana*, *Indian J. Fibre Text. Res.*, 32 (3), 366–372.

[13] dos Santos, G.C., Mendonça, L.M., Antonucci, G.A., dos Santos, A.C., Antunes, L.M.G.A., and Bianchi, M.L.P., 2012, Protective effect of bixin on cisplatin-induced genotoxicity in PC12 cells, *Food Chem. Toxicol.*, 50 (2), 335–340.

[14] Venugopalan, A., Giridhar, P., and Ravishankar, G.A., 2011, Food, ethanobotanical and diversified applications of *Bixa orellana* L.: A scope for its improvement through biotechnological mediation, *Indian J. Fundam. Appl. Life Sci.*, 1 (4), 9–31.

[15] Gómez-Ortíz, N.M., Vázquez-Maldonado, I.A., Pérez-Espadas, A.R., Mena-Rejón, G.J., Azamar-Barrios, J.A., and Oskam, G., 2010, Dye-sensitized solar cells with natural dyes extracted from achiote seeds, *Sol. Energy Mater. Sol. Cells*, 94 (1), 40–44.

[16] Hiendro, A., Hadari, F., Rahmalia, W., and Wahyuni, N., 2012, Enhanced performance of bixin-sensitized TiO_2 solar cells with activated kaolinite, *IJERI*, 4 (1), 40–44.

[17] Ruiz-Anchondo, T., Flores-Holguín, N., and Glossman-Mitnik, D., 2010, Natural carotenoids as nanomaterial precursors for molecular photovoltaics: A computational DFT study, *Molecules*, 15 (7), 4490–4510.

[18] Olson, M., and Allen, N.D., 2012, *Natural photodynamic agents and their use*, Patent, EP2214495A4.

[19] Montenegro, M.A., Rios, A.O., Mercadante, A.Z., Nazareno, M.A., and Borsarelli, C.D., 2004, Model studies on the photosensitized isomerization of bixin, *J. Agric. Food Chem.*, 52 (2), 367–373.

[20] Rios, A.O., Borsarelli, C.D., and Mercadante, A.Z., 2005, Thermal degradation kinetics of bixin in an aqueous model system, *J. Agric. Food Chem.*, 53 (6), 2307–2311.

[21] Kohno, Y., Inagawa, M., Ikoma, S., Shibata, M., Matsushima, R., Fukuhara, C., Tomita, Y., Maeda, Y., and Kobayashi, K., 2011, Stabilization of a hydrophobic natural dye by intercalation into organo-montmorillonite, *Appl. Clay Sci.*, 54 (3-4), 202–205.

[22] Rahmalia, W., 2009, Synthesis of kaolinite-bixin organoclay and their photostability test, *Thesis*, Magister of Biology, Christian University of Satya Wacana, Salatiga, Indonesia.

[23] Picot, P.A., and Grenouillet, P., 1995, Safety in the Chemistry and Biochemistry Laboratory, Eds. Prokopetz, A.T., and Walters, D.B., Wiley-VCH, Inc., New York.

[24] Portejoie, S., Martinez, J., and Landmann, G., 2002, L'ammoniac d'origine agricole: Impacts sur la santé humaine et animale et sur le milieu naturel, *INRA Prod. Anim.*, 15 (3), 151–160.

[25] Tundo, P., and Selva, M., 2002, The chemistry of dimethyl carbonate, *Acc. Chem. Res.*, 35 (9), 706–716.

[26] Rahmalia, W., Fabre, J.F., and Mouloungui, Z., 2015, Effect of cyclohexane/acetone ratio on bixin extraction yield by accelerated solvent extraction method, *Procedia Chem.*, 14, 455–464.

[27] Rahmalia, W., Fabre, J.F., Usman, T., and Mouloungui, Z., 2014, Aprotic solvents effect on the UV-visible absorption spectra of bixin, *Spectrochim. Acta, Part A*, 131, 455–460.

[28] Glukhovsky, V.D., Rostovskaja, G.S., and Rumyna, G.V., 1980, High strength slag alkaline cement, *Proceedings of the 7th International Congress on the Chemistry of Cement*, Paris, 3, 164–168.

[29] Steinerova, M., 2010, Microporous inorganic polymers based on metakaolinite and their open porosity structure of 10-20 nm in diameter, *The 2nd International Conference NANOCON 2010*, Olomouc, Czech Republic, 12–14 October 2010.

[30] Li, C., Sun, H., and Li, L., 2010, A review: The comparison between alkali-activated slag (Si + Ca) and metakaolin (Si + Al) cement, *Cem. Concr. Res.*, 40 (9), 1341–1349.

[31] Freundlich, H., 1906, Adsorption in solution, *Z. Phys. Chem.*, 57, 385-470.

[32] Langmuir, I, 1916, The constitution and fundamental properties of solids and liquids, Part I. Solids, *J. Am. Chem. Soc.*, 38 (11), 2221–2295.

[33] Lagergren, S., 1898, About the theory of so-called adsorption of soluble substances, *Kungl. Svenska Vetenskapsakad. Handl.*, 24 (4), 1–39.

[34] Ho, Y.S., and McKay, G., 1999, Pseudo-second order model for sorption processes, *Process Biochem.*, 34 (5), 451–465.

[35] Vimonses, V., Lei, S., Jin, B., Chow, C.W.K., and Saint, C., 2009, Adsorption of congo red by three Australian kaolins, *Appl. Clay Sci.*, 43 (3-4), 465–472.